www.rericjournal.ait.ac.th

Performance of an Empty Dryer Electrically Heated by Natural and Mixed Convection

Samah Adjmi*,1 and Chérifa Abid+

ARTICLE INFO

Article history:
Received 24 April 2021
Received in revised form
15 October 2021
Accepted 21 October 2021

Keywords:
Absorber
Enthalpy balances
Heat flux
Indirect dryer
Mixed convection
Natural convection

ABSTRACT

In this paper, we report an experimental study on an empty dryer. The device under is an indirect dryer electrically heated. The focus is made on the thermal and fluid behavior in such systems without considering the drying process. Thus, the temperature and fluid velocity profiles are presented in order to determine the fluid flow and the thermal profiles inside the different parts of the dryer in the situations of natural and mixed convection in order to describe and allow a better comprehension of the heat and fluid flow patterns inside a dryer. The enthalpy balances lead to the determination of the most efficient zone in the dryer, this latter is located at 2/3 of its length.

1. INTRODUCTION

A dryer is a device that removes moisture from food to the surrounding exterior. Several literatures were reported on designs and performances of solar dryers [1]. Sharma *et al.* [2] presented a review of solar drying systems where both passive and active modes for various types (direct, indirect, mixed) are considered; El Hage *et al.* [3] carried out a review on solar drying techniques with low environmental and economic impact. In order to see the efficiency of some solar driers, Shobhana *et al.* [4] built direct, indirect and mixed modes solar dryers working in natural and forced convection, they developed correlations for heat transfer at the absorber for the different models and then compared them with the experimental results where they found a good agreement. Musembi *et al.* [5] studied the performance of an indirect solar dryer focusing on the influence of some parameters such the product color on drying process and quality of products to be dried. Sreekumar *et al.* [6] developed a solar dryer with a total volume of 0.272m^3 to investigate its performance; they concluded that their models are more efficient than the traditional one in the conservation of the product original color. Pangavhane *et al.* [7] evaluated the thermal performance of a solar dryer at the absorber and drying chamber in the case of a natural convection heat transfer mode by comparison with an open solar dryer. Demissie *et al.* [13] conducted a numerical and an experimental study on an indirect solar dryer, they investigated the velocity field of the flow in the drying chamber; they showed that the velocity is not uniform at the first floor, varying between 0.25 to 0.08 m/s while it becomes uniform from the second floor with an average velocity around 0.12 m/s. The absorber zone of a dryer can be considered as a differentially heated open channel at both ends, thus some experimental and numerical studies have been made on the heat and mass transfer through a differentially heated open channel [8]-[10]. Ambarita *et al.* [14] studied numerically by CFD code a heat transfer and fluid flow in a flat plate type solar collector with different inclination angles (30, 45, 60 and 70°), the study was done for a naturel convection in a square enclosure heated and cooled from side walls, they found that the average heat transfer coefficient decreases with increasing inclination angle.

In the present study, an experimental study of an empty dryer was evaluated to describe heat and mass flow for natural and mixed convection modes; to the best of our knowledge the mixed convection phenomenon has not been considered before in drying process. The considered system consists of an inclined channel heated from below coupled with a rectangular drying chamber opened at the outlet zone to evacuate the air. The experimental device is instrumented by sensors in order to measure the velocity and temperature profiles in the dryer; the average heat transfer coefficients are determined and compared with correlations. The objective of this paper is to calculate the enthalpic balance, it has been undertaken to determine the most efficient zone of the dryer during the process. Otherwise, the fluid flow and temperature profiles in both convection modes (natural and mixed) were compared in order to provide a better comprehension of the fluid and thermal process in such dryer.

*Chadli Bendjedid University, LPCM, El Tarf, 36000, Algeria.

+Aix Marseille University, CNRS, IUSTI, Marseille, France.

1Corresponding author;
Tel: + 213 657 298 128.
E-mail: adjmisameh@yahoo.fr

2. EXPERIMENTAL SETUP

2.1 Presentation of the Dryer

The experimental dryer is schematically illustrated in Figure 1. The studied system consists of an inclined channel coupled with a vertical rectangular drying chamber, open at both sides, the inlet for the admission and the outlet for the evacuation of the air. The experimental device is widely instrumented to trace fluid velocity and temperature profiles at various locations of the system.

The rectangular channel inclined at 45° plays the role of the absorber, its lower wall is uniformly heated by Joule effect. The heated zone is constituted by the superposition of three layers: the first layer consists of a sheet of polycarbonate of a thickness of 20 mm, the second one corresponds to the heating layer where three adhesive resistances (films) are pasted on the polycarbonate sheet each film has a length of 20 cm, the third layer is a copper plate with a thickness of 10 mm. Thus, the polycarbonate allows the insulation of the lower part of the absorber while the copper contributes to the homogenization of the temperature of the lower wall of the absorber. The other walls of the absorber (the upper and vertical ones) are made of plexiglass of a thickness of 10 mm.

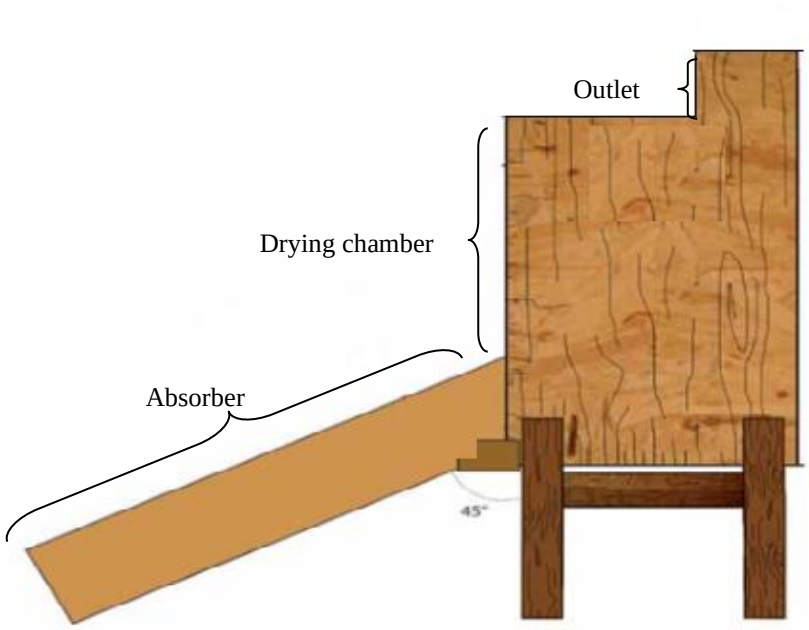

(a). Schematic of the dryer.

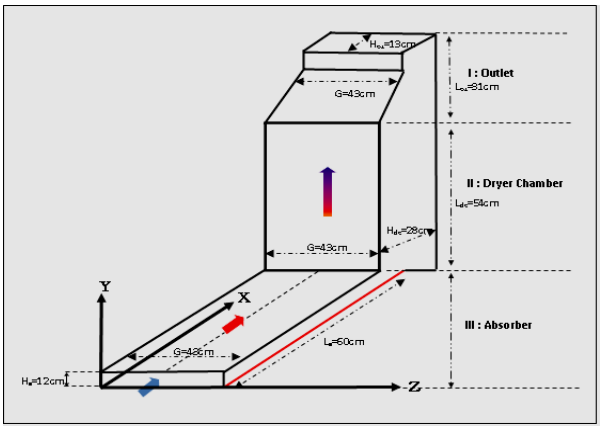

(b). Schematic of the different dimensions

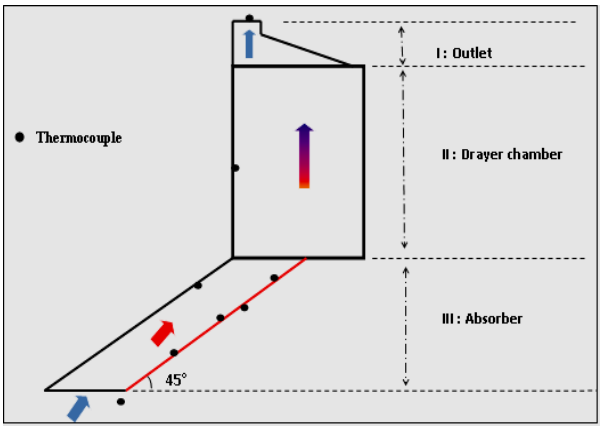

(c). Sensors location

Fig. 1. Schematic representation of the dryer.

The drying chamber and the outlet zone are made of wood plates with a thickness of 5 mm. Table 1 shows the dimensions of the various parts constituting the dryer.

In order to investigate the performance of the system, this later has been equipped with temperature and velocity sensors. For the temperature measurements, eight (K-type)

thermocouples are placed in various locations, as shown on Figure 1-c:

- A thermocouple is placed inside the absorber to measure air temperature (in the center of the absorber),
- Three thermocouples are pasted on the upper part of the heated plate,
- A thermocouple was placed on the rear part of the heated plate which corresponds to the exterior of the lower face of the absorber,
- Three thermocouples are placed inside the absorber (x/L_a=0.85), the drying chamber (y/L_{dc}=0.64) and the outlet zone (z/G=0.5).
- The velocity measurements: The air velocity is measured by two various sensors, depending on the magnitude of the velocity as shown on Table 2.

All the sensors are connected to Labview Signal Express acquisition module.

Table 1. General dimensions of dryer.

Parts of dryer	Dimensions (LxGxH) (cm)
Absorber	60x43x12
Drying chamber	54x43x28
Outlet	31x43x13

Table 2. Sensors used in experimental setup.

Sensor	Type	Number	Signal range	Accuracy
Thermocouple	K	08	0-100°C	±0,1°C
Velocity sensor	HD103T.0	01	0,05-5m/s	±0,04m/s
Velocity sensor	HD29V371TC1.2	01	0,2-20m/s	±0,03m/s

2.2 Settings

Before proceeding to the various experiments, we first achieve the calibration of the various sensors involved in the experiment set-up.

For each experiment, we firstly heated the lower wall of the absorber by Joule effect, indeed the three heating plates of an electrical resistance of 70,7 Ω are submitted to a voltage of 118,9 V. The steady state is obtained after 30 minutes. Then, we proceed to the measurement of velocity and temperature in the three zones of the dryer: absorber 0<y/Ha<1, drying chamber 0.2<x/Hdc<0.95 and outlet zone 0<x/Hoz<1.

3. EXPERIMENTAL RESULTS

3.1 Natural Convection Flow

In the first mode, the heat transfer between the fluid and the absorber is only due to natural convection; the ratio Gr/Re2, determined further is around 75. Figure 2 shows the velocity and temperature profiles inside the absorber. we observe due to the non-slipping condition that the velocity is equal to zero at the horizontal plates of the absorber (y/H_a=0 for the upper face and y/H_a=1 for the lower and heated face of the absorber). In the air Gap, between both the plates, the velocity increases from zero at y/H_a=1 to reach a maximum at y/H_a=0.58, then it decreases progressively till zero at y/H_a=0. This profile is due to natural convection phenomenon, indeed when the working fluid is heated by the hot plate of the absorber, air density decreases which provokes the fluid motion thanks to buoyancy forces, the natural convection is set-up. The temperature profile is plotted on the same figure, and one notices that it is coherent with the velocity one, the highest temperature is found at y/Ha=1, *i.e.* at the heated wall the lowest one is obtained at the same location where the highest velocity was obtained, *i.e.* y/Ha=0.58. When the fluid leaves the absorber, it naturally enters the drying chamber where it goes up along the wall adjacent to the absorber. The measurements conducted in the dryer chamber, allow plotting the horizontal profile of the velocity. It should be noted that the fluid, close to the wall adjacent to the absorber, at x/H_{dc} = 0.2 has the highest velocity (0.35 m/s) and gradually as the x/H_{dc} increases the velocity decreases until it vanishes when x/H_{dc} is around 0.6; beyond this value, there is a quiescent zone without any fluid motion. The temperature profile is approximately uniform around a mean value of 31°C. The same behavior is observed at the outlet area.

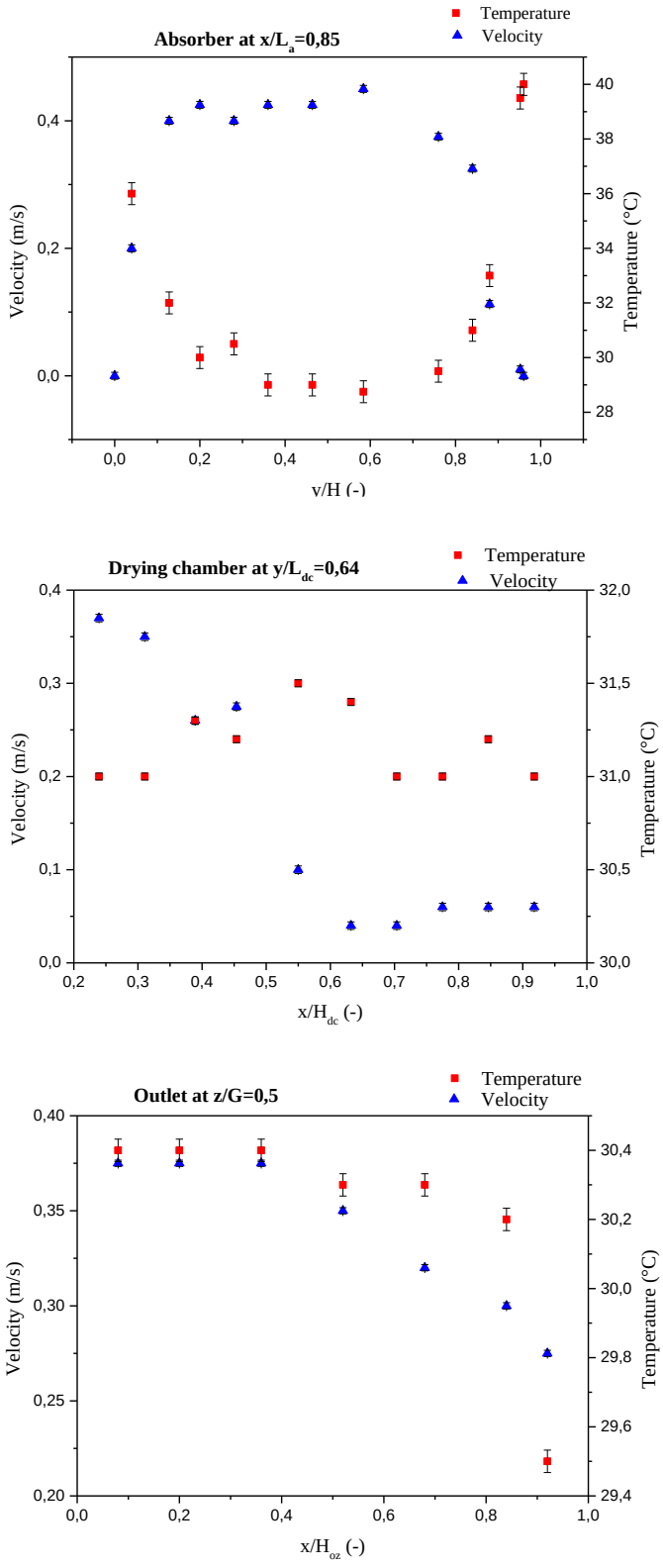

Fig. 2. Velocity and temperature profiles in natural convection dryer.

3.2 Mixed Convection Flow

In the case of mixed convection, the fluid flow is ensured thanks to three fans, submitted to a voltage of 04V installed at the outlet of the dryer. The imposed pressure difference induces a forced flow from the absorber to the outlet. The further determination of the ratio Gr/Re^2 will allow the classification of the type of the involved convection, in this case Gr/Re^2 is around 15, which corresponds to a mixed convection phenomenon.

The various measurements allow to plot the velocity and temperature profiles and to compare them with the case of natural convection.

Thus, Figures 3 and 4 show the velocity and temperature profiles at the absorber and the drying chamber for the same locations as in the case of natural convection.

In the absorber (Figure 3), globally the shape of the curves is the same in both modes, however one can notice that the velocity in the case of mixed convection is larger the highest value is around 0.82 m/s, while it is around 0.41 m/s for the case of natural convection. Otherwise, the profile seems approximately parabolic in mixed convection while it is rather flat in the central zone for natural convection. In the drying chamber, the mixed convection manifests higher profile and one observes that the quiescent zone occurs at greater x/h = 0.7 instead of x/H=0.6 in natural convection which means that the static zone is smaller in mixed convection.

The temperature profiles in the absorber have approximately the same shape even if the fluid temperature is higher in natural convection than in mixed convection, this is due to the residence time of the fluid in the heated zone, indeed, as the velocity is smaller in natural convection, the residence time is larger, which allows to the fluid to be warmer in natural convection than in mixed convection. However, in the drying chamber, the temperature profile is rather flat, *i.e.* the temperature is approximately uniform in natural convection. Moreover, as the velocity is weak the various fluid layers have the same residence time which leads to an uniform temperature. In mixed convection, as the velocity profile is parabolic, the temperature profile behaves symmetrically *i.e.*, its shape is also parabolic.

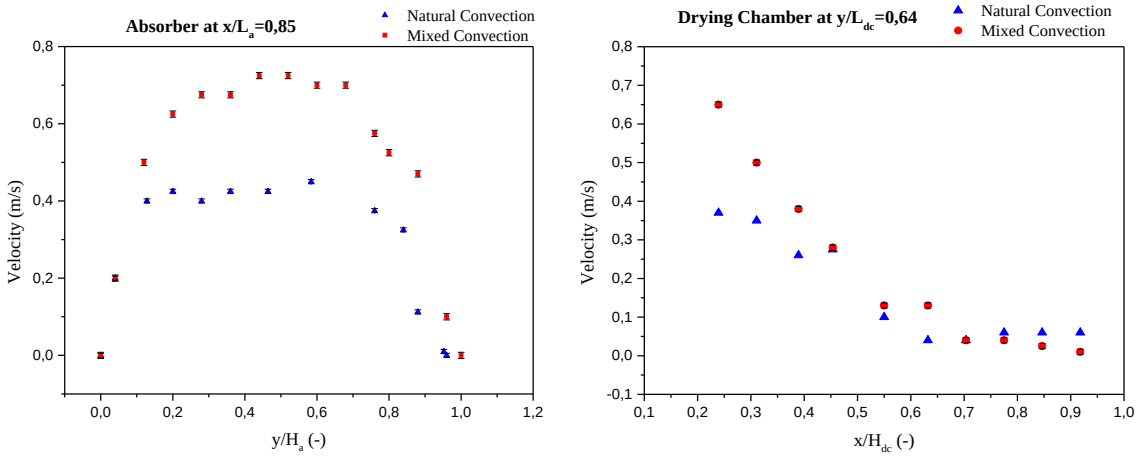

Fig. 3. Comparison of velocity profiles at the absorber and the drying chamber for both heat transfer modes.

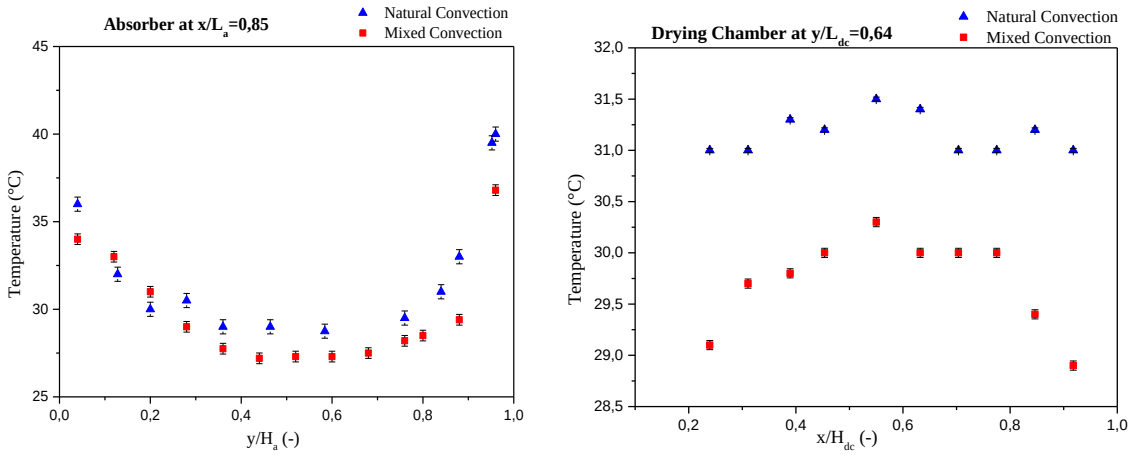

Fig. 4. Comparison of temperature profiles at the absorber and the drying chamber for both heat transfer modes.

4. ENTHALPY BALANCES

4.1 Natural Convection

4.1.1 At the absorber

To understand the thermo-hydraulic mechanisms, it is important to achieve the enthalpy balances at the absorber for both convection modes; in our case, the absorber is an inclined channel heated from below.

For the following, one can determine the heat flux at the inlet φ_{in} and the heat flux at the outlet ϕ_{out} at the absorber. The heat flux at the inlet φ_{in} is defined as:

$$\varphi_{in=}\frac{Q_{in}}{S} \quad (1)$$

Where: Q_{in} is the flux provided to the lower wall of the absorber and it is given by:

$$Q_{in} = U^2/R \text{ and } S = LxG$$

U is the electric tension; R is the electric resistance; S is the surface of the heated wall. Mass flowrate $\dot{m}$ is given by: $\dot{m}=\rho(y_{i+1}-y_i).z.v_i$. Velocities v_i are measured as a function of y_i where $0\leq y\leq 12$cm. The heat flux density at the exit of this zone ϕ_{out} is given by:

$$\varphi_{out}=\frac{Q_{out}}{S} \quad (2)$$

$$Q_{out}=\dot{m}.cp.(T_s-T_e) \quad (3)$$

T_s is the temperature at the outlet; T_e is the temperature at the inlet. Heat flux lost through the walls ϕ_{losses}:

$$\varphi_{losses}=\frac{Q_{losses}}{S} \quad (4)$$

The thermal resistances of the upper wall made in plexiglass (index *v*) and of the lower wall (index p) were calculated as follows:

$$R_v=\frac{e_v}{\lambda_v.S}\ ;\ R_p=\frac{e_p}{\lambda_p.S} \quad (5)$$

Where: e is the wall thickness

So, the thermal power due to thermal losses is given by: $Q_{losses}=Q_v+Q_p$

$$Q_v=\frac{\Delta T}{R_v}=\frac{(T_v-T_a)}{R_v};\ Q_p=\frac{\Delta T}{R_p}=\frac{(T_{ph}-T_p)}{R_p} \quad (6)$$

With T_a the room temperature; T_{ph}: heated wall temperature.

The various measurements give in the Table 3 the values of the various parameters and heat fluxes for the absorber zone in the case of natural convection mode.

4.1.2 At the drying chamber

The Table 4 below summarizes the enthalpy balance made in the drying chamber in the case of natural convection (NC)

4.2 Mixed Convection

In this mode of heat transfer, three fans placed at the outlet (exhaust air to the outside). We note here that the airflow is twice as strong as with natural convection, so the residence time of the air is reduced to half in mixed convection, and this also justifies the decrease of the temperature in exit of the absorber.

To illustrate, the Table 5 presents a comparison between natural and mixed convection of the anthalpic balance in the drying chamber.

Table 3- Enthalpic balance in the absorber "natural convection".

Parameters		
T_e	(°C)	25.5
T_s	(°C)	32.4
$\dot{m}$	(kg/s)	0.016
φ_{in}	(W/m^2)	775.19
φ_{out}	(W/m^2)	442.63
φ_{losses}	(W/m^2)	284.46

Table 4- Enthalpic balance in the dryer chamber "natural convection".

Parameters		NC
T_e	(°C)	32.4
T_s	(°C)	31.2
$\dot{m}$	(kg/s)	0.016
φ_{in}	(W/m^2)	442.63
φ_{out}	(W/m^2)	113.95
φ_{in}- φ_{out}	(W/m^2)	329.21

Table 5- Enthalpic balance in drying chamber with mixed convection (MC).

Parameters		MC
T_e	(°C)	25.5
T_s	(°C)	29.8
$\dot{m}$	(kg/s)	0.027
φ_{in}	(W/m^2)	775.19
φ_{out}	(W/m^2)	448.07
φ_{in}- φ_{out}	(W/m^2)	251.67

Based on the calculated values of enthalpy balance in absorber, the dimensionless numbers Gr and Re can be calculated as:

- The Grashof number based on ϕ_{out} ou φ_{out} can be obtained by:

$$Gr=\frac{g.\beta.\varphi_{out}.H_a{}^4}{\lambda.\nu^2} \quad (7)$$

- Furthermore, the Reynolds number based on the hydraulic diameter D_H can be expressed as:

$$Re = \frac{2.\dot{m}.D_H}{\rho.\nu.(H_a + G)} \quad (8)$$

Calculation of the average heat transfer coefficient, h_{exp}

$$h_{exp} = \frac{\varphi_{in}}{\Delta T} \quad (9)$$

$$Nu_{exp} = \frac{h_{exp}.H}{\lambda} \quad (10)$$

To compare the experimental Nusselt number in dryer chamber with theory, we consider this zone as an open inclined channel.

In natural convection, the correlation performed by Azevedo and Sparrow [11] for an inclined channel was applied:

$$Nu = 0.645.\left[Ra_S\left(\frac{S}{L}\right)\right]^4 \quad (11)$$

In mixed convection, the empirical correlation of Osborne and Incropera [12] was applied:

$$Nu = 2\left[0.414\ Gz + 0.015(Gr.Pr)^{3/4}\right]^{1/3} \quad (12)$$

Table 6 compares the values of heat transfer coefficient and Nusselt number found experimentally with the correlations mentioned above, one can notice that mixed convection leads to an enhancement of the convective heat transfer which contributes to a better heat exchange. This is due to the helical trajectories of the fluid induced by the combination of a transverse component of velocity due to buoyancy and axial component due to forced flow. This combination leads to longer time of residence of the fluid in the channel.

Table 6. Heat transfer coefficient and Nusselt number.

	h_{exp}	Nu_{exp}	h_{corr}	Nu_{corr}	Error
	($W/K.m^2$)	(-)	($W/K.m^2$)	(-)	(%)
NC	11.01	59.83	10.6	57.14	04.49
MC	12.03	65.39	14.2	76	13

5. CONCLUSION

This article presents the results of an experimental investigation on a system composed of an inclined channel coupled to a rectangular drying chamber attached to an outlet to evacuate the air. The experimental device has certain modularity and allows to vary some parameters or boundary conditions of the system. The instrumentation of the system allows the access to fluid temperature and velocity profiles. This survey was implemented to study the influence of the heat flow distribution at the inclined channel for the chimney effect with natural and mixed convections. The instrumentation allowed us to understand the importance of various thermo-hydraulic mechanisms related to the system parameters. The enthalpic balances were calculated and allowed us to determine the most effective zone in the construction of the solar dryer. Whatever convection and heating modes, we observed heterogeneity of velocities and temperatures within the drying chamber. This consequence could have a negative effect on the homogeneity of the drying quality.

Even, the drying food has not been taken into account, nevertheless the heat transfer mode varying from natural to mixed convection affect the heat and fluid flow pattern which contributes to drying process. The perspective of this work is on one hand to promote mixed convection for a better heat transfer exchange and on the second hand to design the geometry in order to homogenize the temperature in the drying chamber and to take into account the food drying.

NOMENCLATURE

b	absorber clearance (m)
e	plate clearance (m)
G	width (m)
g	gravity acceleration (m/s^2)
Gr	Grashof number (-)
H_a	height of the absorber (m)
H_{dc}	height of the dryer chamber (m)
H_{oz}	height of the outlet zone (m)
l	length of absorber (m)
L_a	length of the absorber (m)
L_{dc}	length of the dryer chamber (m)
L_{oz}	length of the outlet zone (m)
$\dot{m}$	mass flow (kg/s)
Nu	Nusselt number (-)
Pr	Prantl number, $\eta cp/\lambda$
Ra	Rayleigh number, $Ra = Gr.Pr$
Re	Reynolds number (-)
T	temperature (°C)
V, U	velocity (m/s)
α	coefficient of expansion of air
λ	thermal conductivity of air (W/mK)
ν	kinetic viscosity (m^2/s)
φ	heat flux (W/m^2)

REFERENCES

[1] Mustayen A.G.M.B., Mekhilef S., and Saidur R., 2014. Performance study of different solar dryers: A review. *Renewable and Sustainable Energy Reviews* 34: 463–470.

[2] Sharma A., Chen C.R., and Vu Lan N., 2009. Solar-energy drying systems: A review. *Renewable and Sustainable Energy Reviews* 13: 1185–1210.

[3] El Hage H., Herez A., Ramadan M., Bazzi H., and Khaled M., 2018. An investigation on solar draying: A review with economic and environmental assessment. *Energy* 157: 815-829.

[4] Shobhana S. and S. Kumar. 2012. Development of convective heat transfer correlations for common designs of solar dryer. *Energy Conversion and Management* 64: 403–414.

[5] Musembi M.N., Kiptoo K.S., and Yuichi N., 2016. Design and analysis of solar dryer for mid-latitude region, *Energy Procedia* 100: 98 – 110.

[6] Sreekumar A., Manikantan P.E., and Vijayakumar K.P., 2008. Performance of indirect solar cabinet dryer. *Energy Conversion and Management* 49: 1388–1395.

[7] Pangavhane D.R., Sawhney R.L., and Sarsavadia P.N., 2002. Design, development and performance testing of a new natural convection solar dryer. *Energy* 27: 579–590.

[8] Lu Q., Qiu S., Su G., Tian W., and Ye Z., 2010. Experimental research on heat transfer of natural convection in vertical rectangular channels with large aspect ratio. *Experimental Thermal and Fluid Science* 34(1): 73 – 80.

[9] Dupont F., Ternat F., Samot S., and Blonbou R., 2013. Two-dimension experimental study of the reverse flow in a free convection channel with active walls differentially heated. *Experimental Thermal and Fluid Science* 47: 150–157.

[10] Ong K. and C. Chow. 2003. Performance of a solar chimney. *Solar Energy* 74 (1): 1 – 17.

[11] Incropera, DeWitt, Bergman, Lavine; 2006; Fundamentals of Heat and Mass Transfer. Sixth Edition, Chapter 9, P. 587, John Wiley & Sons, United Kingdom.

[12] Osborne D.G. and F.P. Incropera. 1985. Laminar mixed convection heat transfer for flow between horizontal parallel plates with asymmetric heating. *International Journal Heat Mass Transfer* 28: 207-217.

[13] Demissie P., Hayelom M., Kassaye A., Hailesilassie A., Gebrehiwot M., and Vanierschot M. 2019. Design, development and CFD modeling of indirect solar food dryer. *Energy Procedia* 158: 1128–1134.

[14] Ambarita H., Siregari R.E.T., Ronowikarto A.D., and Setyawan E.Y., 2018. Effects of the inclination angle on the performance of flat plate solar collector. *2nd International Conference on Computing and Applied Informatics* 2017. Journal of Physics: Conf. Series 978.